Journal of Alloys and Compounds 509 (2011) 651–655

Contents lists available at ScienceDirect

Journal of Alloys and Compounds

journal homepage: www.elsevier.com/locate/jallcom

Effects of Al and Al_4C_3 contents on combustion synthesis of Cr_2AlC from Cr_2O_3–Al–Al_4C_3 powder compacts

C.L. Yeh*, C.W. Kuo

Department of Aerospace and Systems Engineering, Feng Chia University, 100 Wenhwa Road, Seatwen, Taichung 40724, Taiwan

ARTICLE INFO

Article history:
Received 6 August 2010
Received in revised form 5 September 2010
Accepted 8 September 2010
Available online 20 October 2010

Keywords:
Ceramics
X-ray diffraction
SEM
Cr_2AlC
Combustion synthesis

ABSTRACT

Preparation of the ternary carbide Cr_2AlC was conducted by combustion synthesis in the mode of self-propagating high-temperature synthesis (SHS) from the Cr_2O_3–Al–Al_4C_3 powder compact. Effects of the contents of Al and Al_4C_3 on the product composition and combustion behavior were studied by formulating the reactant mixture with a stoichiometric proportion of Cr_2O_3:Al:Al_4C_3 = 3:5x:y, where x and y varied from 1.0 to 1.5. When compared to those of the powder compact with Cr_2O_3:Al:Al_4C_3 = 3:5:1 (i.e., $x = y = 1.0$), the combustion temperature and reaction front velocity increased with content of Al, but decreased with that of Al_4C_3. Besides Cr_2AlC and Al_2O_3, the final products always contained a secondary phase Cr_7C_3 that was substantially reduced by adopting additional Al and Al_4C_3 in the reactant compacts. For the sample with Cr_2O_3:Al:Al_4C_3 = 3:7.5:1 ($x = 1.5$), solid state combustion reached a peak temperature of 1245 °C and yielded Cr_2AlC with a trivial amount of Cr_7C_3. Although Cr_7C_3 was lessened by introducing extra Al_4C_3, the increase of Al_4C_3 from $y = 1.1$ to 1.5 produced almost no further reduction of Cr_7C_3 in the final product. This is partly attributed to the low combustion temperature in the range of 1065–1095 °C for the samples with additional Al_4C_3, and in part, due to the role of Al_4C_3 which might react with Cr to form Cr_7C_3, Cr_2Al, and Cr_2AlC.

1. Introduction

The $M_{n+1}AX_n$ phases, where $n = 1$, 2, or 3, M is an early transition metal, A is an A-group (mostly IIIA and IVA) element, and X is either C or N, are a class of hexagonal-structure ternary carbides and nitrides which possess many merits of metals and ceramics [1–6]. MAX compounds are typically resistant to oxidation and corrosion, elastically stiff, but at the same time they exhibit high thermal and electrical conductivities and are machinable. These salient properties stem from an inherently laminated crystal structure, within which the $M_{n+1}X_n$ slabs are intercalated by pure A-element layers [6].

Cr_2AlC, a member of the M_2AX ($n = 1$) family, was first discovered by Jeitschko et al. [7] in 1963. Its lattice parameters and phase relationship in the Cr–Al–C system were identified by Schuster et al. [8]. In recent years, Cr_2AlC has received increasing attention because of its remarkable properties, including relatively low hardness, high elastic modulus, high flexural and compression strength, good electric and thermal conductivity, and excellent oxidation and corrosion resistance [9–14]. Fabrication routes like hot pressing [11–16] and pulse discharge sintering [17–19] have been frequently used to prepare bulk Cr_2AlC. Besides, the molten salt method [20] and magnetron sputtering technique [21,22] were used to produce Cr_2AlC in the forms of powders and thin films, respectively.

With an in situ hot pressing/solid–liquid reaction method, Lin et al. [11] produced Cr_2AlC from the Cr, Al, and graphite powders, and proposed the related reaction mechanism with two intermetallic compounds, Cr_2Al and Cr_5Al_8, involving in the formation sequence of Cr_2AlC. A series of hot-pressing investigations was conducted by Tian et al. [13–16] to fabricate Cr_2AlC from the Cr, Al, and graphite powders at 850–1450 °C and 20 MPa for 1 h. It was found that the samples with an additional amount of Al, such as Cr:Al:C = 2:1.2–1.6:1, were beneficial to reduce the secondary phase Cr_7C_3 in the final product [15]. An increase in the hot-pressing temperature enhanced the reaction between Cr_2Al, Cr_5Al_8, Cr, and graphite; therefore, Cr_2AlC without intermediate phases was obtained at temperatures above 1250 °C [16]. Lin et al. [12] utilized chromium carbides (Cr_7C_3 and Cr_3C_2) mixing with Cr and Al powders as the starting materials to produce Cr_2AlC by hot pressing at 1400 °C. In addition, Cr_2AlC was prepared by pulse discharge sintering from the Cr–Al–C [17,18] and Cr–Al_4C_3–C [19] powder mixtures. According to Tian et al. [17,19], two minor phases Cr_7C_3 and Cr_2Al were observed and both of them decreased with increasing sintering temperature.

As a promising alternative method, combustion synthesis in the mode of self-propagating high-temperature synthesis (SHS) takes

* Corresponding author. Tel.: +886 4 24517250x3963; fax: +886 4 24510862.
E-mail address: clyeh@fcu.edu.tw (C.L. Yeh).

0925-8388/$ – see front matter © 2010 Elsevier B.V. All rights reserved.
doi:10.1016/j.jallcom.2010.09.169

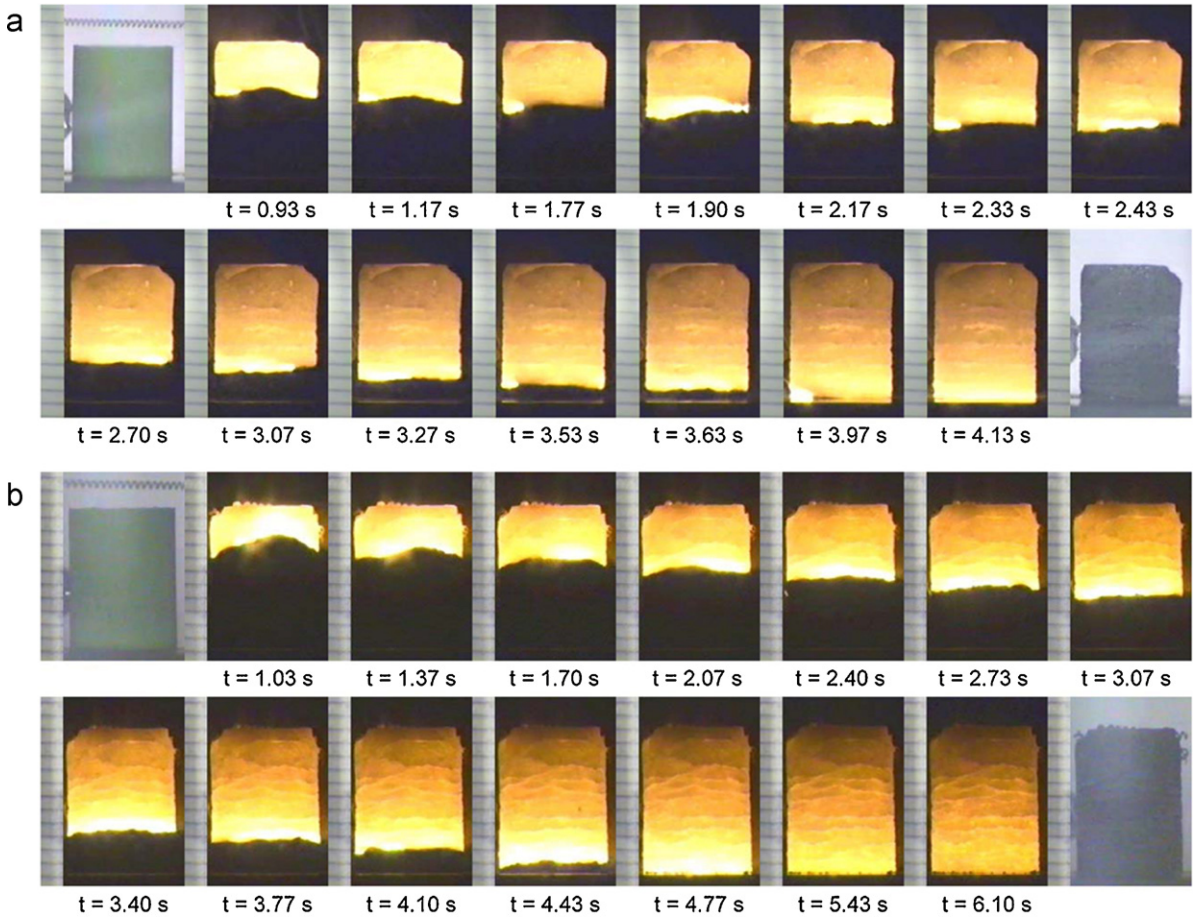

Fig. 1. Typical SHS sequences recorded from solid state combustion of powder compacts of $3Cr_2O_3 + 5xAl + yAl_4C_3$ with (a) $x = 1.5$ and $y = 1.0$, and (b) $x = 1.0$ and $y = 1.2$.

advantage of the self-sustaining merit from highly exothermic reactions, and hence, has the benefits of low energy requirement, short reaction time, and simple facilities [23–26]. The SHS technique has been applied to produce a number of the MAX carbides, like Ti_3SiC_2 [27], Ti_3AlC_2 [28], Ti_2AlC [29], Ta_2AlC [30], Nb_2AlC [31], and Ti_2SnC [32]. However, the formation of Cr_2AlC from its constituent elements by the SHS process is unfeasible, due mostly to insufficient exothermicity of the reactions among Cr, Al, and carbon [33].

In this study, the first attempt was made to prepare Cr_2AlC through combustion synthesis in the SHS mode. Sample compacts are composed of Cr_2O_3, Al, and Al_4C_3 powders. The use of Cr_2O_3 as the source of chromium is to take advantage of the thermal energy released from the thermite reaction between Cr_2O_3 and Al to sustain self-propagating combustion [34]. Moreover, the by-product Al_2O_3 generated from the thermite reaction is recognized as an excellent reinforcement for the MAX carbides to improve their hardness, toughness, and strength [35,36]. In particular, effects

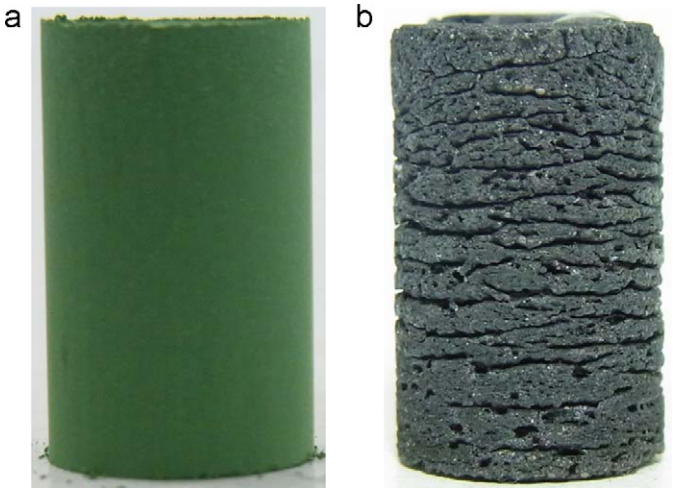

Fig. 2. Photographs of the $3Cr_2O_3 + 5Al + Al_4C_3$ powder compact: (a) before and (b) after combustion.

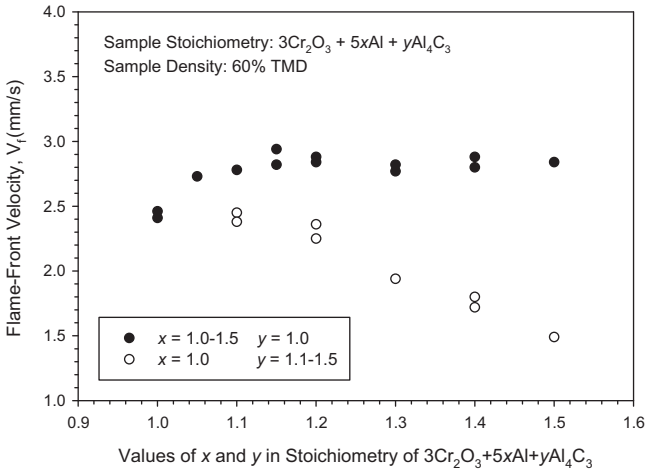

Fig. 3. Effect of Al and Al_4C_3 contents on flame-front propagation velocity of Cr_2O_3–Al–Al_4C_3 powder compacts.

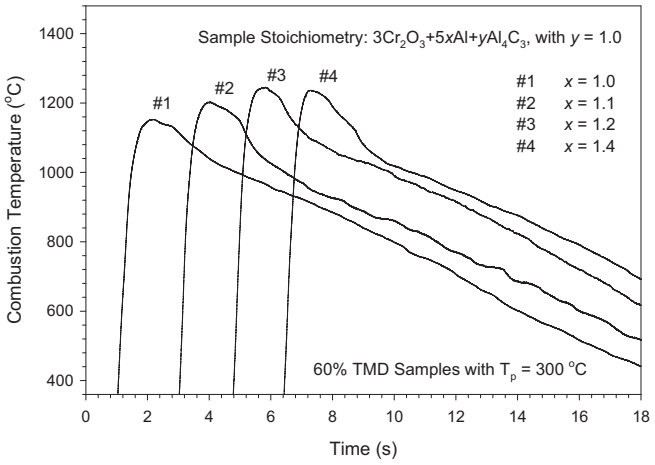

Fig. 4. Effect of Al content on combustion temperature of Cr_2O_3–Al–Al_4C_3 powder compacts.

of the contents of Al and Al_4C_3 are studied on the formation of Cr_2AlC, as well as on the combustion temperature and propagation velocity of the reaction front. The reaction mechanism associated with the formation of Cr_2AlC from solid state combustion in the Cr_2O_3–Al–Al_4C_3 system is also addressed.

2. Experimental methods of approach

Chromium oxide Cr_2O_3 (Showa Chemical Co., 99% purity), aluminum (Showa Chemical Co., <40 μm, 99% purity), and aluminum carbide Al_4C_3 (Strem Chemicals, <45 μm, 98% purity) powders were used as the starting materials to prepare Al_2O_3-added Cr_2AlC in this study. The reaction between Cr_2O_3, Al, and Al_4C_3 under an exact stoichiometric balance was expressed as reaction (1), where Cr_2O_3:Al:Al_4C_3 = 3:5:1.

$$3Cr_2O_3 + 5Al + Al_4C_3 \rightarrow 3Cr_2AlC + 3Al_2O_3 \quad (1)$$

According to the previous studies on the synthesis of Cr_2AlC [15,16], Ta_2AlC [30], Ti_2AlC [37], and Ti_3AlC_2 [38], it was suggested that an off-stoichiometric composition with additional Al was favorable for the evolution of end products. Therefore, the reactant powders of this study were formulated at Cr_2O_3:Al:Al_4C_3 = 3:5*x*:*y*, where the stoichiometric parameters *x* and *y* varied from 1.0 to 1.5. This means that additional aluminum from either elemental Al or Al_4C_3 is explored.

Reactant powders were dry mixed in a ball mill and then cold-pressed into the cylindrical sample compacts with a diameter of 7 mm, a height of 12 mm, and a compaction density of 60% relative to the theoretical maximum density (TMD). The SHS experiments were conducted in a stainless-steel windowed combustion chamber under an atmosphere of high purity argon (99.99%). The sample holder was equipped with a 600 W cartridge heater used to raise the initial temperature of the sample prior to ignition. A preheating temperature (T_p) of 300 °C was required by this study to assure self-sustaining combustion of the Cr_2O_3–Al–Al_4C_3 powder compacts. Details of the experimental setup and measurement approach were reported elsewhere [39]. The microstructure of synthesized products was examined under a scanning electron microscope (Hitachi S3000H), and phase composition was analyzed by an X-ray diffractometer (Bruker D8SSS) with Cu Kα radiation.

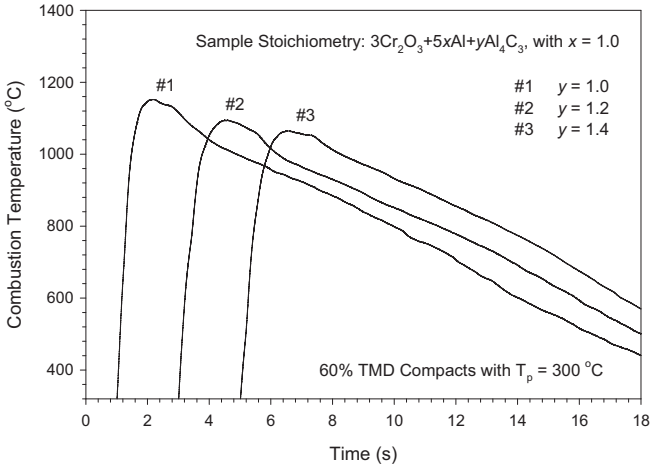

Fig. 5. Effect of Al_4C_3 content on combustion temperature of Cr_2O_3–Al–Al_4C_3 powder compacts.

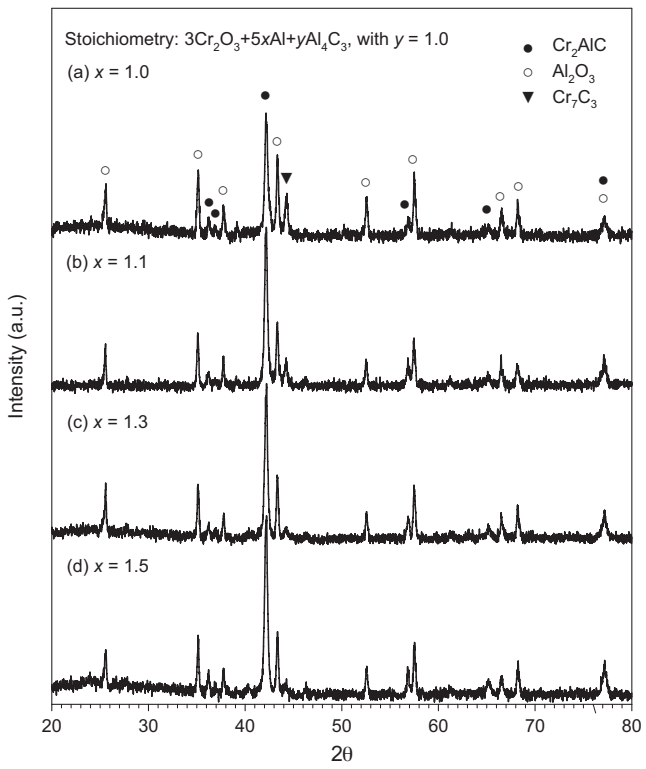

Fig. 6. XRD patterns of products synthesized from combustion of powder compacts of $3Cr_2O_3 + 5xAl + yAl_4C_3$ with *y* = 1.0 and *x* = (a) 1.0, (b) 1.1, (c) 1.3, and (d) 1.5.

3. Results and discussion

3.1. Observation of combustion characteristics

Two typical SHS sequences illustrating solid state combustion of the Cr_2O_3–Al–Al_4C_3 powder compacts with different starting compositions are presented in Fig. 1(a) and (b), both of which feature one localized reaction zone propagating spirally along the sample in a self-sustaining manner. According to Ivleva and Merzhanov [40], once the heat flux released from self-sustaining combustion is no longer sufficient to maintain steady propagation of a planar front, combustion inclines to be restricted within one or several hot spots spreading along the sample. Therefore, Fig. 1(a) and (b) reflects the weak reaction exothermicity of the Cr_2O_3–Al–Al_4C_3 samples and justify the need of prior heating up to 300 °C on the reactant compact.

Fig. 2 displays the photographs of a $3Cr_2O_3 + 5Al + Al_4C_3$ powder compact before and after combustion. The unburned sample shown in Fig. 2(a) has a smooth surface and is green due to the color of Cr_2O_3. As illustrated in Fig. 2(b), the sample turns out to be dark grey after combustion and exhibits spiral marks on its rugged exterior because of the propagation of the spinning combustion wave.

3.2. Measurement of flame-front propagation velocity and combustion temperature

The flame-front propagation velocity (V_f) in the axial direction was determined from the recorded combustion images and plotted in Fig. 3 as a function of the starting stoichiometry of the reactant compact. The flame-front velocity was found to increase from

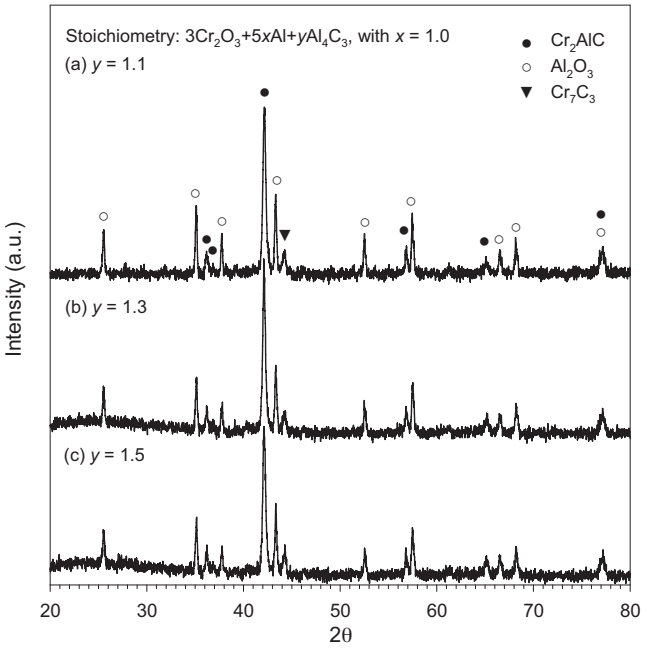

Fig. 7. XRD patterns of products synthesized from combustion of powder compacts of $3Cr_2O_3 + 5xAl + yAl_4C_3$ with $x = 1.0$ and $y =$ (a) 1.1, (b) 1.3, and (c) 1.5.

2.4 to 2.9 mm/s with increasing Al content from $x = 1.0$ to 1.15, beyond which the propagation rate varied within the neighborhood of 2.77–2.88 mm/s. The increase of combustion velocity with Al content was largely caused by an enhancement in the degree of Cr_2AlC formation, which resulted in a higher reaction temperature and hence a faster combustion wave. The nearly constant reaction rate observed for the samples with $x \geq 1.15$ could be a result of the thermal balance between the increase of reaction exothermicity from the Cr_2AlC formation and the loss of more energy as the latent heat of additional Al.

In contrast, Fig. 3 shows that the reaction front is significantly decelerated by increasing the amount of Al_4C_3 in the sample compacts from $y = 1.1$ to 1.5. The lowest combustion propagation rate about 1.5 mm/s was detected from the sample of $3Cr_2O_3 + 5Al + 1.5Al_4C_3$. The decrease of the flame-front velocity is attributed to a decrease in the overall reaction exothermicity caused probably by the consumption of additional energy to decompose extra Al_4C_3 during the SHS process.

Combustion temperature profiles measured from test samples of different starting compositions are depicted in Figs. 4 and 5, accounting respectively for the influence of extra amounts of Al and Al_4C_3. The abrupt rise in the temperature curve signifies rapid arrival of the combustion wave and the peak value corresponds to the reaction front temperature. Most importantly, the composition dependence of the combustion temperature presented in Figs. 4 and 5 is consistent with that of the reaction front velocity shown in Fig. 3. As indicated in Fig. 4, the increase of the Al content from $x = 1.0$ to 1.2 led to an increase in the combustion front temperature from 1150 to 1245 °C, but comparable peak temperatures were observed for the samples with $x = 1.2$ and 1.4.

On the other hand, Fig. 5 shows a decrease in the combustion temperature with increasing Al_4C_3 content. The reaction front temperatures of the samples with excessive Al_4C_3 at $y = 1.2$ and 1.4 are about 1095 and 1065 °C, respectively. As reported by Tian et al. [16,19], the reaction temperature favoring the formation of Cr_2AlC has to be higher than 950 °C for the Cr–Al–C sample and 1050 °C for the Cr–Al_4C_3–C sample. Based upon the combustion temperatures presented in Figs. 4 and 5, the exothermicity of the Cr_2O_3–Al–Al_4C_3 powder compact for the evolution of Cr_2AlC is justified.

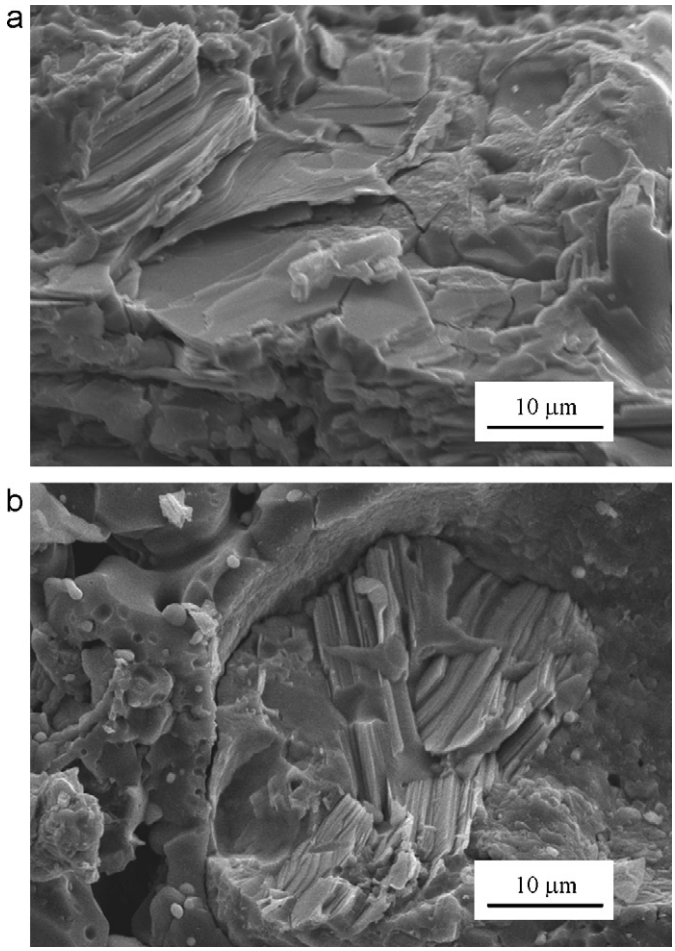

Fig. 8. SEM micrographs illustrating fracture surfaces of products synthesized from powder compacts of $3Cr_2O_3 + 5xAl + yAl_4C_3$ with (a) $x = 1.4$ and $y = 1.0$, and (b) $x = 1.0$ and $y = 1.2$.

3.3. Phase constituent and morphology of combustion products

Fig. 6(a)–(d) plots XRD patterns of the final products obtained from samples containing different amounts of elemental Al. In addition to the by-product Al_2O_3 and the binary carbide Cr_7C_3, the as-synthesized product is dominated by Cr_2AlC. The presence of Cr_7C_3 as a minor phase has been commonly reported in the fabrication of Cr_2AlC [13–19]. As indicated in Fig. 6(a)–(d), the content of Cr_7C_3 is greatly reduced when the green compact contains additional Al. For the Al-rich sample at $x = 1.5$, the XRD spectrum of Fig. 6(d) reveals a negligible amount of Cr_7C_3 in the end product. This confirms an improvement in the evolution of Cr_2AlC by a supplementary amount of Al involving in the reaction. The added Al was mainly to compensate for the evaporation of Al during the combustion process at temperatures higher than its melting point, which is in agreement with the synthesis of Ta_2AlC [30], Ti_2AlC [37], and Ti_3AlC_2 [38].

It is believed that solid state combustion of the Cr_2O_3–Al–Al_4C_3 system is initiated by the thermite reaction of Al with Cr_2O_3:

$$2Al + Cr_2O_3 \rightarrow 2Cr + Al_2O_3 \quad (2)$$

With the reaction heat released from reaction (2), the reaction of reduced Cr with Al was triggered and the intermetallic compound Cr_2Al was formed as reaction (3). At the same time, the interactions between Cr and Al_4C_3 occurred according to reactions (4) and (5).

$$2Cr + Al \rightarrow Cr_2Al \quad (3)$$

$$8Cr + Al_4C_3 \rightarrow 3Cr_2AlC + Cr_2Al \quad (4)$$

$$15Cr + Al_4C_3 \rightarrow 4Cr_2Al + Cr_7C_3 \quad (5)$$

Formation of Cr_2AlC, Cr_2Al, and Cr_7C_3 was observed in reactions (4) and (5). Although Cr_2Al is absent in the final product, this Cr–Al aluminide has been identified as an important intermediate for the production of Cr_2AlC [11,16,17,19]. During the SHS process, Cr_2Al could react with Cr, Cr_7C_3, and Al_4C_3 to form Cr_2AlC as reaction (6).

$$Cr + 2Cr_2Al + Cr_7C_3 + Al_4C_3 \rightarrow 6Cr_2AlC \quad (6)$$

The influence of Al_4C_3 content on the phase composition of final products is presented in Fig. 7(a)–(c). When compared with the product of the $3Cr_2O_3 + 5Al + Al_4C_3$ sample ($y = 1.0$) shown in Fig. 6(a), the sample with a slightly extra amount of Al_4C_3 at $y = 1.1$ contains less Cr_7C_3 phase. However, Fig. 7(b) and (c) indicates that no further reduction of Cr_7C_3 was achieved by adopting more Al_4C_3 in the reactant compacts, partly because Al_4C_3 could react with Cr to yield Cr_7C_3 through reaction (5). In addition, the decrease of the reaction temperature with increasing Al_4C_3 produced an adverse effect on the evolution of Cr_2AlC.

Fig. 8(a) and (b) represents typical SEM micrographs on the fracture surface of synthesized products. As can be seen in Fig. 8(a), the plate-like grains of Cr_2AlC are closely stacked into a laminated structure. The layered structure characteristic of the ternary MAX carbide is also clearly observed in Fig. 8(b).

4. Conclusions

Preparation of the ternary carbide Cr_2AlC was achieved by combustion synthesis in the SHS mode from the sample compact composed of Cr_2O_3, Al, and Al_4C_3 powders. In the SHS process, the thermite reaction of Al with Cr_2O_3 not only acts as the initiating step, but also produces Al_2O_3 as a reinforcement for Cr_2AlC. When compared with the exact stoichiometric proportion of Cr_2O_3:Al:Al_4C_3 = 3:5:1, the off-stoichiometric composition with extra Al or Al_4C_3 causes the variations of combustion temperature and reaction velocity and improves the evolution of Cr_2AlC.

Experimental evidences showed that increasing the content of Al from $x = 1.0$ to 1.15 in the sample of Cr_2O_3:Al:Al_4C_3 = 3:5x:1 led to an increase in combustion temperature and thus a faster reaction front. However, both combustion temperature and flame velocity remained almost unchanged for the samples with initial Al in the range of $x = 1.2$–1.5, due most likely to comparable reaction exothermicity. Besides Al_2O_3, the as-synthesized product is composed of Cr_2AlC along with Cr_7C_3 as the secondary phase. The content of Cr_7C_3 in the final product was noticeably reduced by increasing Al. Consequently, the optimum product with a trivial amount of Cr_7C_3 was obtained from the sample of Cr_2O_3:Al:Al_4C_3 = 3:7.5:1 ($x = 1.5$).

Because Al_4C_3 represents another source of Al in the Cr_2O_3–Al–Al_4C_3 powder compact, the need of additional Al can be implemented by increasing the content of Al_4C_3. It was found that combustion temperature and flame-front velocity decreased with increasing content of Al_4C_3 from $y = 1.0$ to 1.5 in the proportion of Cr_2O_3:Al:Al_4C_3 = 3:5:y. As the content of Al_4C_3 is higher than the stoichiometric amount ($y = 1.0$), the secondary phase Cr_7C_3 in the final product is reduced. However, the degree of Cr_7C_3 reduction by increasing Al_4C_3 is not as effective as that by adopting additional Al.

Acknowledgement

This research was sponsored by the National Science Council of Taiwan, ROC, under the grant of NSC 98-2221-E-035-065-MY2.

References

[1] M.W. Barsoum, Prog. Solid State Chem. 28 (2000) 201–281.
[2] M.W. Barsoum, D. Brodkin, T. El-Raghy, Scr. Mater. 36 (5) (1997) 535–541.
[3] M.W. Barsoum, T. El-Raghy, J. Am. Ceram. Soc. 79 (7) (1996) 1953–1956.
[4] J.Y. Wang, Y.C. Zhou, Annu. Rev. Mater. Res. 39 (2009) 415–443.
[5] H.B. Zhang, Y.W. Bao, Y.C. Zhou, J. Mater. Sci. Technol. 25 (2009) 1–38.
[6] P. Eklund, M. Beckers, U. Jansson, H. Högberg, L. Hultman, Thin Solid Films 518 (2010) 1851–1878.
[7] W. Jeitschko, H. Nowotny, F. Benesovsky, Monatsh. Chem. 94 (4) (1963) 672–676.
[8] J.C. Schuster, H. Nowotny, C. Vaccaro, J. Solid State Chem. 32 (1980) 213–219.
[9] Z.J. Lin, Y.C. Zhou, M.S. Li, J. Mater. Sci. Technol. 23 (6) (2007) 721–746.
[10] D.B. Lee, T.D. Nguyen, J. Alloys Compd. 464 (2008) 434–439.
[11] Z.J. Lin, Y.C. Zhou, M.S. Li, J.Y. Wang, Z. Metallkd. 96 (3) (2005) 291–296.
[12] Z.J. Lin, M.S. Li, J.Y. Wang, Y.C. Zhou, Acta Mater. 55 (2007) 6182–6191.
[13] W.B. Tian, P.L. Wang, G.J. Zhang, Y.M. Kan, Y.X. Li, D.S. Yan, Scr. Mater. 54 (2006) 841–846.
[14] W.B. Tian, P.L. Wang, G.J. Zhang, Y.M. Kan, Y.X. Li, J. Am. Ceram. Soc. 90 (2007) 1663–1666.
[15] W.B. Tian, P.L. Wang, G.J. Zhang, Y.M. Kan, Y.X. Li, D.S. Yan, Mater. Sci. Eng. A 454–455 (2007) 132–138.
[16] W.B. Tian, P.L. Wang, Y.M. Kan, G.J. Zhang, Y.X. Li, D.S. Yan, Mater. Sci. Eng. A 443 (2007) 229–234.
[17] W.B. Tian, K. Vanmeensel, P.L. Wang, G.J. Zhang, Y.X. Li, J. Vleugels, O. Van der Biest, Mater. Lett. 61 (2007) 4442–4445.
[18] W.B. Tian, Z.M. Sun, Y.L. Du, H. Hashimoto, Mater. Lett. 63 (2009) 670–672.
[19] W.B. Tian, Z.M. Sun, Y.L. Du, H. Hashimoto, Mater. Lett. 62 (2008) 3852–3855.
[20] W.B. Tian, P.L. Wang, Y.M. Kan, G.J. Zhang, J. Alloys Compd. 461 (2008) L5–L10.
[21] J.M. Schneider, Z. Sun, R. Mertens, F. Uestel, R. Ahuja, Solid State Commun. 130 (2004) 445–449.
[22] C. Walter, D.P. Sigumonrong, T. El-Raghy, J.M. Schneider, Thin Solid Films 515 (2006) 389–393.
[23] A.G. Merzhanov, J. Mater. Process. Technol. 56 (1996) 222–241.
[24] Z.A. Munir, U. Anselmi-Tamburini, Mater. Sci. Rep. 3 (1989) 277–365.
[25] C.L. Yeh, in: K.H.J. Buschow, R.W. Cahn, M.C. Flemings, E.J. Kramer, S. Mahajan, P. Veyssiere (Eds.), Encyclopaedia of Materials: Science and Technology, Elsevier, Amsterdam, 2010.
[26] C.L. Yeh, in: M. Lackner (Ed.), Combustion Synthesis—Novel Routes to Novel Materials, Bentham Science, 2010.
[27] C.L. Yeh, Y.G. Shen, J. Alloys Compd. 461 (2008) 654–660.
[28] C.L. Yeh, Y.G. Shen, J. Alloys Compd. 473 (2009) 408–413.
[29] C.L. Yeh, Y.G. Shen, J. Alloys Compd. 470 (2009) 424–428.
[30] C.L. Yeh, Y.G. Shen, J. Alloys Compd. 482 (2009) 219–223.
[31] C.L. Yeh, C.W. Kuo, J. Alloys Compd. 496 (2010) 566–571.
[32] C.L. Yeh, C.W. Kuo, J. Alloys Compd. 502 (2010) 461–465.
[33] M. Binnewies, E. Milke, Thermochemical Data of Elements and Compounds, Wiley-VCH Verlag GmbH, Weinheim, New York, 2002.
[34] L.L. Wang, Z.A. Munir, Y.M. Maximov, J. Mater. Sci. 28 (1993) 3693–3708.
[35] J.X. Chen, Y.C. Zhou, Scr. Mater. 50 (2004) 897–901.
[36] H.J. Wang, Z.H. Lin, Y. Miyamoto, Ceram. Int. 28 (2002) 931–934.
[37] W.B. Zhou, B.C. Mei, J.Q. Zhu, X.L. Hong, Mater. Lett. 59 (2005) 131–134.
[38] Y. Zou, Z.M. Sun, H. Hashimoto, S. Tada, J. Alloys Compd. 456 (2008) 456–460.
[39] C.L. Yeh, Y.L. Chen, J. Alloys Compd. 478 (2009) 163–167.
[40] T.P. Ivleva, A.G. Merzhanov, Doklady Phys. 45 (2000) 136–141.